# Chimeric Thermostable DNA Polymerases with Reverse Transcriptase and Attenuated 3′−5′ Exonuclease Activity

Nancy J. Schönbrunner,* Ellen H. Fiss, Olga Budker, Susanne Stoffel, Christopher L. Sigua,‡ David H. Gelfand, and Thomas W. Myers

*Program in Core Research, Roche Molecular Systems, Inc., 1145 Atlantic Avenue, Alameda, California 94501*

*Received May 8, 2006; Revised Manuscript Received August 2, 2006*

ABSTRACT: The synthesis of accurate, full-length cDNA from low-abundance RNA and the subsequent PCR amplification under conditions which provide amplicon that contains minimal mutations remain a difficult molecular biological process. Many of the challenges associated with performing sensitive, long RT/PCR have been alleviated by using a mixture of DNA polymerases. These mixtures have typically contained a DNA polymerase devoid of 3′−5′ exonuclease, or "proofreading", activity blended with a small amount of an *Archaea* DNA polymerase possessing 3′−5′ exonuclease activity, since reverse transcriptases lack 3′−5′ exonuclease activity and generally have low fidelity. To create a DNA polymerase with efficient reverse transcriptase and 3′−5′ exonuclease activity, a family of mutant DNA polymerases with a range of attenuated 3′−5′ exonuclease activities was constructed from a chimeric DNA polymerase derived from *Thermus* species Z05 and *Thermotoga maritima* DNA polymerases. These "designer" DNA polymerases were fashioned using structure-based tools to identify amino acid residues involved in the substrate-binding site of the exonuclease domain of a thermostable DNA polymerase. Mutation of some of these residues resulted in proteins in which DNA polymerase activity was unaffected, while proofreading activity ranged from 60% of the wild-type level to undetectable levels. Kinetic characterization of the exonuclease activity indicated that the mutations affected catalysis much more than binding. On the basis of their specificity constants ($k_{cat}/K_M$), the mutant enzymes have a 5−15-fold stronger preference for a double-stranded mismatched substrate over a single-stranded substrate than the wild-type DNA polymerase, a desirable attribute for RT/PCR. The utility of these enzymes was evaluated in a RT/PCR assay to generate a 1.7 kb amplicon from HIV-1 RNA.

The process of polymerase chain reaction (PCR) has become increasingly important in nucleic acid-based diagnostics and molecular biology research in general. However, performing sensitive, long (more than ∼1 kb) PCR has remained a problematic and time-consuming procedure, especially in the clinical laboratory setting. One critical issue in the sensitive synthesis of full-length cDNA and subsequent PCR amplification is nucleotide misincorporation by the reverse transcriptase and/or DNA polymerase (DNA pol).[1] Such events lead not only to a decrease in fidelity but also to reduced extension from the 3′ mismatch, and thus reduced efficiency of cDNA synthesis and DNA amplification (*1*). Although nucleotide misincorporation for most reverse transcriptases and DNA polymerases is generally infrequent [$5 \times 10^{-4}$ for HIV-1 reverse transcriptase (*2*) and $1 \times 10^{-5}$ for *Thermus aquaticus* DNA pol (*Taq* pol) (*3*−*5*)], even relatively low misincorporation rates could significantly impair amplification of long targets. The low fidelity of reverse transcriptases leads to decreased amounts of full-length cDNA being produced. Thus, the enzymatic removal of nucleotides misincorporated by the reverse transcriptase and/or DNA polymerase could significantly improve the efficiency of the reactions.

The thermostable DNA polymerases most widely used in PCR to date belong to the pol A family of enzymes, but they lack proofreading activity. One approach to achieving sensitive long RT and/or PCR amplification is to use a mixture of thermostable DNA polymerases in a single-buffer system (*1*, *6*). These mixtures contain a DNA polymerase devoid of 3′−5′ exonucleolytic activity blended with a low level of a DNA polymerase exhibiting proofreading activity. The proofreading activity is responsible for editing misincorporated nucleotides (*7*) and is typically derived from an *Archaea* family B DNA polymerase, such as from *Thermococcus litoralis* [Vent pol (*8*)], *Pyrococcus* species GB-D [Deep Vent pol (*9*)], or *Pyrococcus furiosus* [*Pfu pol* (*5*)]. One problem with this approach is that the *Archaea* DNA polymerases are inhibited by dUMP-containing template, therefore precluding the utilization of dUTP and subsequent uracil-*N*-glycosylase (UNG) treatment for the prevention of carryover contamination (*10*−*12*). While the inclusion of a

* To whom correspondence should be addressed. Telephone: (510) 814-2906. Fax: (510) 814-2910. E-mail: nancy.schoenbrunner@roche.com.

‡ Current address: Celera Diagnostics, 1401 Harbor Bay Parkway, Alameda, CA 94502.

[1] Abbreviations: DNA pol, DNA polymerase; *Taq*, *Thermus aquaticus*; *Tma*, *Thermotoga maritima*; *T.* Z05, *Thermus* species Z05; *Tth*, *Thermus thermophilus*; FAM, 6-carboxyfluorescein; KOAc, potassium acetate; DMSO, dimethyl sulfoxide; $Mn(OAc)_2$, manganese acetate; EDTA, ethylenediaminetetraacetic acid; DTT, dithiothreitol; Tris, tris(hydroxymethyl)aminomethane; Tricine, *N*-[tris(hydroxymethyl)methyl]-glycine; PEG, polyethylene glycol; TAPS, *N*-tris(hydroxymethyl)-methyl-3-aminopropanesulfonic acid.

10.1021/bi0609117 CCC: $33.50 
Published on Web 10/03/2006

proofreading DNA polymerase may improve the fidelity and efficiency of reverse transcription and/or PCR amplification (*5*, *13*), high levels of proofreading activity have detrimental effects on PCR amplification efficiency (*6*). In addition, high levels of proofreading may lead to degradation of the primers present in the PCR amplification mix. Primer degradation due to 3′−5′ exonucleolytic activity on the single-stranded DNA substrate leads to loss of the ability of the primer to specifically hybridize to its intended target sequence. Additionally, excessive proofreading activity can lead to nonproductive idling reactions and can negatively affect the integrity of the 3′ terminus of the newly synthesized DNA following strand separation and preceding primer hybridization. To circumvent the problem of primer degradation, two approaches have been implemented: (1) the use of only low levels of proofreading activity in the blend of DNA polymerases and (2) covalent modifications at or near the 3′ terminus of primers to protect them from nonspecific 3′−5′ exonucleolytic attack (*14*, *15*). Ideally, such modifications should not impact the ability of the DNA polymerase to efficiently use the primers for template-directed extension.

An alternative approach to the blending of DNA polymerases is the modulation of the 3′−5′ exonucleolytic activity in a family A enzyme by means of mutagenesis. Family A DNA polymerases are multidomain, multifunction enzymes. The N-terminal domain possesses 5′ nuclease activity, and the C-terminal domain possesses the DNA polymerase activity. The intervening domain catalyzes 3′−5′ exonucleolysis. In some DNA polymerases, for example *Taq* (*16*, *17*), *Thermus thermophilus* (*Tth*) (*18*), or *Thermus* species *Z05* (*19*, *20*), the activity is effectively absent due to significant mutations and loop deletions in that domain (*21*).

Considerable research has been done on the *Escherichia coli* DNA polymerase I (*E. coli* pol I) (*22*, *23*). The Klenow fragment of *E. coli* pol I contains two enzymatic activities, the DNA polymerase and the 3′−5′ exonuclease. A number of structures of the Klenow fragment with either the dNMP product or single-stranded DNA substrate bound to the 3′−5′ exonuclease active site have been described, and a two-metal ion catalytic mechanism has been proposed for the 3′−5′ exonuclease (*15*, *24*−*28*). One metal ion (metal ion A) positions the substrate and activates the water for nucleophilic attack. The water or $OH^-$ nucleophile is further oriented in the active site by the side chains of Glu325 and Tyr464. The trigonal bipyramidal transition state is stabilized by both metals. The second metal ion (metal ion B) is also proposed to stabilize the negative charge that builds up on the leaving 3′ oxygen (*29*). The DNA substrate observed in the cocrystal structures is single-stranded. It is proposed that the single-stranded DNA either binds directly to the 3′−5′ exonuclease active site or is derived from the frayed end of duplex DNA bound to the DNA polymerase domain and is shuttled to the 3′−5′ exonuclease active site. However, most of the structural and functional characterizations of family A DNA polymerase 3′−5′ exonucleases have been carried out with enzymes derived from *E. coli* and other mesophilic organisms. To the best of our knowledge, there have been no reports on the crystal structure of the 3′−5′ exonuclease domain of thermostable family A DNA polymerases.

To design thermophilic DNA polymerases with modulated proofreading activity, we took advantage of the extensive structural knowledge already reported for the Klenow fragment. We used the structure described by Brautigam et al. [PDB entry 1kfs (*15*)] in which the Klenow fragment was cocrystallized with standard phosphodiester single-stranded DNA as a template to model the unknown structure of the highly homologous *Thermotoga maritima* DNA pol (*Tma* pol) (*30*) 3′−5′ exonuclease domain. This high-resolution (2.1 Å) structure is particularly well suited to serve as a template for homology modeling, given the fact that it represents the wild-type form of the enzyme and that both metals were unambiguously identified. Furthermore, this cocrystal was apparently freeze-trapped in a precatalytic state. Similar methods were used by Villbrandt et al. (*31*) as part of a study to design chimeras of *Thermotoga neopolitana* and *Taq* DNA pol, but those chimeric proteins were not thermostable.

In this study, we identified amino acid residues in the 3′−5′ exonuclease domain of the modeled structure of *Tma* pol predicted to be involved in substrate binding or catalysis. We utilized a chimeric DNA polymerase, termed CS5 pol, which had been previously constructed from *T.* Z05 pol and *Tma* pol and contained the 5′−3′ nuclease domain from *T.* Z05 pol (residues 1−291) and the 3′−5′ exonuclease and polymerase domains from *Tma* pol (residues 292−893) (*32*). This chimera retained thermostable DNA polymerase activity, as well as proofreading activity. Using the CS5 chimera, we then made a series of mutant proteins in which the amino acid side chains were mutated to modulate the 3′−5′ exonuclease activity. These new enzymes were evaluated for DNA polymerase activity and 3′−5′ exonuclease activity on a variety of substrates. We also describe here the first thermoactive and thermostable enzyme with reverse transcriptase and 3′−5′ exonuclease activity, as well as the use of these thermostable mutant DNA polymerases in RT/PCR.

## EXPERIMENTAL PROCEDURES

*Oligonucleotides*. Oligonucleotides were synthesized and purified using a 394 DNA/RNA synthesizer (Applied Biosystems, Foster City, CA) and conventional solid phase $\beta$-cyanoethyl phosphoramidite chemistry (*33*). For the direct 5′ end labeling of oligonucleotides with fluorescent dyes, 6-carboxyfluorescein (FAM) phosphoramidites (Biogenix, San Ramon, CA) were used.

*Structure-Based Design of Mutations.* For the design of proofreading mutants, a homology model of the proofreading domain of the *Tma* pol was created on the basis of the 2.1 Å resolution structure of the Klenow fragment of *E. coli* pol I cocrystallized with single-stranded DNA [PDB entry 1kfs (*15*)]. Sequences were aligned with the X-Windows Sequence Alignment Editor [XSAE (*34*)]. Model building was performed with Moloc (*35*) implemented on a Silicon Graphics Indy workstation. Insertions and deletions were modeled by a loop of suitable length and subjected to an initial energy minimization with all other atoms constrained. The final model was subjected to a restrained energy minimization.

*Construction of Mutant DNA Polymerases*. Plasmids pCS5 and pCS6, encoding chimeric DNA polymerases, were utilized in the site-directed mutagenesis. The pCS5 and pCS6 plasmids were constructed from *T.* Z05 and *Tma* and contained the 5′−3′ nuclease domain from *T.* Z05 pol (residues 1−291) and the 3′−5′ exonuclease and polymerase domains from *Tma* pol (residues 292−485 and 486−893,

respectively). Chimera CS6 is a mutant of CS5 pol in which amino acids D323 and E325 were replaced with alanines to completely destroy the 3′−5′ exonuclease activity. The first set of mutations, round one, targeted residues 323−325 (L324E/D/K/H/N/Q, D323E, E325D, or D323E/E325D). These mutations were generated by digesting the pCS6 plasmid with the restriction enzymes *Spe*I and *Sgf*I to remove the sequence encoding residues 323−325 and replacing them by ligation with the following oligonucleotide pairs: 5′-TGACCTGGATA-3′ and 5′-CTAGTATCCAGCTCAAT-3′ for E325D, 5′-TGAGCTTGAGA-3′ and 5′-CTAGTCTCAAGCTCAAT-3′ for D323E, and 5′-TGAGCTGGATA-3′ and 5′-CTAGTATCCAGCTCAAT-3′ for D323E/E325D. The oligonucleotide pairs, in addition to containing the modified bases for the amino acid changes, also contained silent base changes for introduction of new unique restriction sites. For the L324 amino acid changes, the following oligonucleotides were used: 5′-CGACGAAGAGA-3′ and 5′-CTAGTCTCTTCGTCGAT-3′ for L324E, 5′-CGACGATGAGA-3′ and 5′-CTAGTCTCATCGTCGAT-3′ for L324D, 5′-TGATAAGGAAA-3′ and 5′-CTAGTTTCCTTATCAAT-3′ for L324K, 5′-TGATCAGGAAA-3′ and 5′-CTAGTTTCCTGATCAAT-3′ for L324Q, 5′-CGATAATGAAA-3′ and 5′-CTAGTTTCATTATCGAT-3′ for L324N, and 5′-CGATCATGAAA-3′ and 5′-CTAGTTTCATGATCGAT-3′ for L324H. For this set, the oligonucleotides for L324D and L324E were pooled. Similarly, the oligonucleotides for L324Q and L324K or L324N and L324H were pooled, and after cloning had been carried out, the correct amino acid changes were identified by the unique restriction sites as well as by DNA sequencing.

Round two mutants were generated by PCR-mediated site-directed mutagenesis (*36*) to create amplicons with the desired amino acid change and a silent diagnostic restriction enzyme site incorporated near the change. The amplicon contained unique restriction sites allowing for insertion of the new sequence into the pCS5 plasmid, which had been cut by the same restriction enzymes. For generation of the L329A mutant, one amplification was required, whereas two overlapping amplifications were required to generate the additional mutations. The following primers were utilized: L329A, forward primer CS20 (5′-GAAACTAGTTCC*GCT*-GATCCTTTCGA-3′) and reverse primer CS36 (5′-GAAAA-GAGAAGGACATGAGCTCTTGGTAA-3′); Y464A, forward primers CS21 (5′-AGAAAAAGCTGCGAAT-*GCA*TCCTGTGAAGATGCAGA-3′) and CS35 (5′-ACCAA-*GAGCTC*ATGTCCTTCTCTTTTCCG-3′) and reverse primers CS22 (5′-CTGCATCTTCACAGGA*TGC*ATTCGCAGC-TTTTTCTA-3′) and CS37 (5′-TTTCCAGATCTGCC-TCGTGGAGTTTTAA-3′); Q384A, forward primers CS23 (5′-CGTTGGT*GCC*AATTTGAAATTCGATTACAA-3′) and AW964 (5′-GGAAACTAGTTCCCTCGATCC-3′) and reverse primers CS24 (5′-TGTAATCGAATTTCAAATT*G-GC*ACCAACGA-3′) and CS36; N385A, forward primers CS25 (5′-CGTTGGTCAG*GCC*TTGAAATTCGATTACAA-3′) and AW964 and reverse primers CS26 (5′-TGTAATC-GAATTTCAA*GGC*CTGACCAACGA-3′) and CS36; Q384A/N385A, forward primers CS27 (5′-CGTTGGT*GCCGC*T-*C*TGAAATTCGATTACAA-3′) and AW964 and reverse primers CS28 (5′-TGTAATCGAATTTCA*GAGCGGC*AC-CAACGA-3′) and CS36; D389E, forward primers CS29 (5′-TGAAATTCGA*G*TACAAGGTGTTGATGGTGAA-3′) and AW964 and reverse primers CS30 (5′-CAACACCTTG-TA*C*TCGAATTTCAAA-3′) and CS36. The mutated codons are italicized. The PCR-amplified fragments were cloned into the pCS5 vector at the *Spe*I and *Sac*I sites for L329A, D389E, Q384A, N385A, and Q384A/N385A and the *Bgl*II and *Sac*I sites for Y464A. Mutations were constructed in a high-level expression plasmid for protein expression. For each mutant that was constructed, the mutated amplicon was first screened by restriction analysis as each new mutation also contained a new restriction site. The amplicon was ligated into the CS5 plasmid in which the wild-type sequence had been removed by restriction digestion and gel purification. The new construct was transformed by electroporation into the host cells and the sequence of the new DNA polymerase confirmed by sequencing.

*Purification of DNA Polymerases*. The pCS5 plasmid and its derivatives were transformed into *E. coli*. The chimeric DNA polymerases were overexpressed under the control of the lambda $P_L$ promoter. Five hundred milliliters of cells was grown and heat induced, and proteins were purified to near homogeneity using previously published procedures (*37*). The protein concentrations were determined by quantitation of the appropriate Coomassie-stained bands following polyacrylamide gel electrophoresis.

*DNA Polymerase and 3′−5′ Exonuclease Assays.* The DNA polymerase activity was assayed as described previously (*17*) under the following conditions at 74 °C: 25 mM TAPS (pH 9.4), 50 mM KCl, 2 mM $MgCl_2$, dGTP, dATP, and TTP (200 $\mu$M each), and 100 $\mu$M [$\alpha$-$^{33}$P]dCTP at 190−240 cpm/pmol. One unit of DNA polymerase activity is defined as the amount of enzyme that incorporates 10 nmol of TCA-precipitatable DNA product in 30 min. The 3′−5′ exonuclease activity was determined by measuring the rate of removal of the 3′ terminal nucleotide from a 5′ fluorescently labeled synthetic oligonucleotide substrate. This substrate oligonucleotide [NJS40 (5′-FAM-GCGCTA-GGGCGCTGGCAAGTGTAGCGGTCAC-3′)] was a unique, nonrepeating sequence and was either single-stranded or annealed to a perfectly matched oligonucleotide template [NJS43 (5′-CCGCGGCGGGTGTGGTGGTTACGCGCAG-CGTGACCGCTACACTTGCCAGCGCCCTAGCGAP-3′)] or to an oligonucleotide providing a mismatch to the 3′ terminus of the primer [NJS44 (5′-CCGCGGCGGGTGTG-GTGGTTACGCGCAGCTTGACCGCTACACTTGCC-AGCGCCCTAGCGAP-3′)]. The underlined nucleotides indicate the template to the 3′ terminal dC of the primer. The reactions (40 $\mu$L) were performed at 63 °C, and the mixtures were comprised of 4 pmol of FAM-labeled oligonucleotide in 50 mM Tricine (pH 8.3), 25 mM KOAc, 5% (w/v) DMSO, and 0.5 mM $Mn(OAc)_2$. To mimic PCR conditions, the reaction mixtures also contained a 5% contribution from enzyme storage buffer to give 1 mM Tris (pH 8.0), 5 mM KCl, 5.0 $\mu$M EDTA, 0.025% Tween 20, 0.05 mM DTT, and 2.5% (v/v) glycerol. Reactions were initiated by addition of oligonucleotide substrate and divalent metal to the enzyme solution and quenched after 15 min by EDTA (final concentration of 50 mM). The fragments were separated by capillary electrophoresis (ABI PRISM 3100, Applied Biosystems). The relative amounts of the full-length and degraded oligonucleotides were quantitated by GENESCAN (Applied Bioystems).

The quantity of oligonucleotide converted to shorter oligonucleotide products is equal to

$$[1\text{-}(\textit{relative } P_n)]*(\text{pmol of } P_n \text{ at the start of reaction})$$

where $P_n$ is the substrate oligonucleotide of initial length $n$ and relative $P_n$ is equal to the fluorescence intensity of $P_n$ divided by the sum of fluorescent intensities of all detected fragments. One unit of 3′−5′ exonuclease activity is defined as the amount of enzyme that catalyzes the conversion of 50 pmol of NJS40 oligonucleotide to shorter oligonucleotides in 15 min. Enzyme concentrations were adjusted to ensure the linearity of the assay (2.5−50 pM for the wild-type enzyme). Calculated rates were normalized to an enzyme concentration of 0.25 nM.

*Steady-State Kinetics.* A modified version of the assay employing a 5′-FAM-labeled oligonucleotide substrate with a 3′ homopolymer tail [NJS98 (5′-FAM-TAACCTCGTCAGAGCAGACCAGAGCAAAAAAAAAAAAAAA-3′)] was used to determine the kinetic parameters of 3′−5′ exonucleolysis. The oligonucleotide was either single-stranded or annealed to a complementary template [NJS99B (5′-TCCAACCAAC*UUUUUUUUUUUUUUU*GCTCTGGTCTGCTCTGACGAGGTTGP-3′)]. The template contained propynyl-dU, indicated by *U*, opposite dA to increase the stability of the duplex ($T_M$ = 73 °C) and ensure complete hybridization at the assay temperature of 63 °C, as indicated by melting curves (data not shown). Reactions were otherwise carried out as described above.

The quantity of total degradation product is equal to

$$(\text{relative } P_{n-x})*X*(\text{pmol of } P_n \text{ at start of reaction})$$

where $P_{n-x}$ is the degradation product of length $n-x$ and $X$ is the number of phosphodiester bonds cleaved to generate $P_{n-x}$. This assay was used to measure the cumulative rate of phosphodiester bond cleavage, considering shorter oligonucleotides as both product and substrate for subsequent reactions. The rates were linear for degradation of up to 12 nucleotides. Initial rates were determined by least-squares analysis, and the $k_{cat}$ and $K_M$ values were extrapolated from a Lineweaver−Burke double-reciprocal plot using Grafit (Erithacus Software, Ltd., Surrey, U.K.).

*RT/PCR Amplification.* The enzymes were tested for RT/PCR activity using a HIV-1 transcript RNA target. The 100 μL PCR mixture contained 50 mM Tricine (pH 8.3), 45 mM KOAc (pH 7.5), 0.9 mM $Mn(OAc)_2$, 5% (w/v) DMSO, 0.75% PEG 10K, dATP, dGTP, and dCTP (200 μM each), 300 μM dUTP, 30 μM TTP, 200 nM primers RN326 (5′-GAGGGGTATTGACAAACTCCCACTCAGGAATC*C*A-3′) and RN328 (5′-GGGAATTTTCTTCAGAGCAGACCAGAGCCAA*C*A-3′) where *C* is 2′-amino-dC, and 1 unit of UNG. The DNA polymerase used was either a blend of proofreading-proficient (CS5) and -deficient (CS6) chimeric parent enzymes or the modulated proofreading DNA polymerases. The PCR conditions were as follows: 50 °C for 2 min, 60 °C for 60 min, and 95 °C for 1 min, followed by four cycles of 95 °C for 20 s, 58 °C for 15 s, and 65 °C for 105 s, followed by 36 cycles of 90 °C for 20 s, 58 °C for 15 s, and 65 °C for 105 s using an Applied Biosystems 9600 DNA thermal cycler (Applied Biosystems). The RT/PCR products were analyzed by electrophoresis on an agarose gel stained with ethidium bromide.

## RESULTS

*Structure-Based Design of Mutations.* In these studies, we used the chimeric protein, CS5 pol. The CS5 pol is a fusion of two proteins, the 5′−3′ exonuclease domain from *T.* Z05 pol (residues 1−291), and the 3′−5′ exonuclease and pol domains from *Tma* pol (residues 292−485 and 486−893, respectively). Replacement of the complete 5′ nuclease domain from *Tma* pol with that from *T.* Z05 pol led to improved protein expression (data not shown). The 3′−5′ exonuclease domain from *Tma* pol is homologous to the same domain from *E. coli* pol I (51.9 and 33.7% similar and identical in sequence, respectively). Using the cocrystal structure of the Klenow fragment as a template to construct a model (*38*) of the *Tma* pol proofreading domain in CS5 pol, the putative 3′−5′ exonuclease active site was identified on the basis of three conserved sequence motifs: Exo I, II, and III (*39*). These motifs comprise the critical residues that define the substrate binding pocket and active site and are highly conserved between *E. coli* pol I and *Tma* pol. There are only three insertions or deletions, all fewer than three amino acids in length, in the alignment between *E. coli* pol I and *Tma* pol, none of which occur within conserved motifs. The Klenow fragment thus serves as a very reliable template for building a model of the unknown *Tma* pol proofreading domain. The quality of the inferred structural model of the chimera's proofreading domain was high as judged by the 3D profile scores (*40*, *41*). Large, positive scores (>20 for a sliding 21-residue segment) indicate that the amino acid residues are in their preferred environment in terms of solvent exposure, secondary structure, and occlusion by polar and hydrophobic atoms. A 3D profile score below zero would indicate potential problems in that region of the structural model. The average 3D profile score for the inferred model structure of CS5 pol was virtually identical to that of the Klenow cocrystal structure (40.0 and 40.7, respectively). In only one region, centered on residues 443−451, did the sliding average 3D profile score drop below 10 (Figure 1a). However, none of these loop residues are found near the active site. This loop in Tma pol is longer by two residues and contains more hydrophobic amino acids than the homologous loop in *E. coli* pol I.

The modeled structure of CS5 pol was used to select residues for mutation by molecular modeling criteria (Figure 1b,c). These included amino acids with atoms <5 Å from the DNA substrate or metal and that interact favorably with the DNA or metal, based on calculated van der Waals and hydrogen bonding energies. All identified residues were implicated in the catalysis or substrate binding of the 3′−5′ exonuclease activity. They are shown graphically in Figure 1 and outlined in Table 1. The residues were categorized using the convention of Derbyshire et al. (*42*) for the *E. coli* Klenow fragment as metal ligators, substrate contacts at the 3′ terminus, or upstream contacts with the substrate sugar−phosphate backbone.

*Construction and Purification of the Mutants of CS5 pol.* Using standard site-directed mutagenesis methods (see Experimental Procedures), we mutated the sites listed in Table 1. The amino acid substitutions were designed with

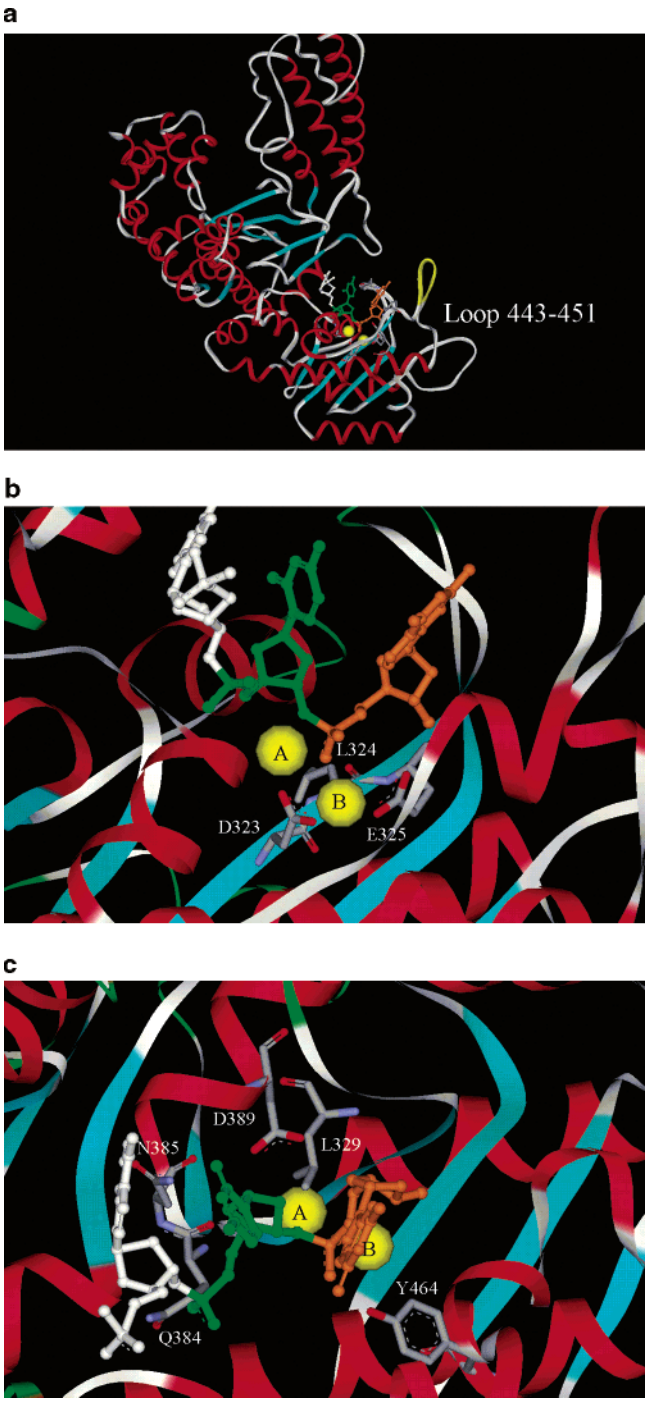


FIGURE 1: Modeled structure of the 3′−5′ exonuclease active site of the CS5 chimeric DNA polymerase highlighting residues identified for mutagenesis. The protein is displayed as a ribbon colored by secondary structure (red for α-helix, cyan for *β*-sheet, and white for loop). The two metal ions are shown as yellow space-filling spheres (metal ion A is a Zn and metal ion B is a Mg). The three bases of the DNA substrate are shown as ball-and-stick diagrams colored orange, green, and white. (a) Loop defined by residues 443−451 in *Tma* pol showing the lowest 3D profile score and therefore likely greatest differences with respect to the mesophilic homologue Klenow fragment. (b) Residues 323−325. D323 and E325 chelate metal ion A, while L324 points away from the active site. (c) Residues distal from the scissile phosphodiester bond. For the proposed function of the individual residues, see Table 1.

the intention of diminishing but not completely destroying the activity.

*3′−5′ Exonuclease Activity of Mutants.* All proteins were assayed in a buffer optimized for RT/PCR with moderate monovalent salt and low divalent metal ion concentrations and a temperature of 63 °C. Since this assay examines the rate of removal of only the 3′ terminal nucleotide from a nonrepeating sequence, it allows the determination of activity for the same sequence context on both a 3′-matched and mismatched duplex, as well as on a single-stranded oligonucleotide. Activity was measured at oligonucleotide concentrations of 100 nM to approximate the concentration of primer used in a typical PCR amplification. Under these conditions, wild-type chimera CS5 pol displayed approximately the same degradation rates with the single-stranded and matched duplex substrates (9.9 and 11.3 units/pmol, respectively) and an almost 2-fold higher degradation rate (16.6 units/pmol) with the terminally mismatched duplex.

The 3′−5′ exonuclease activity for each mutant enzyme was observed to be reduced by varying degrees (Table 2). Mutations to the metal ligating class of residues were differentially tolerated. Mutations of the carboxylates that directly chelate metal ion A (D323E or E325D) resulted in complete elimination of 3′ exonuclease activity, while the analogous mutation of the metal ion B ligator (D389E) led to a partial activity reduction.

Mutations to the second class of residues, i.e., those found near the 3′ terminus of the DNA substrate, also resulted in quite disparate results. The phenolic OH group of Tyr464 interacts with the *pro-R* oxygen of the scissile phosphodiester bond. Replacement of Y464 with alanine eliminated 3′-exonuclease activity completely. The second residue of this class that was examined in this study, Leu324, is located between the essential caboxylates that ligate metal ion A. Although its backbone atoms are near the active site, its side chain points away from the active site (Figure 1). We mutated the small, neutral side chain to a number of charged or polar residues. Such mutations resulted in a very modest reduction in 3′−5′ exonuclease activity (27−67% residual activity, depending upon the nature of the substrate and mutation). Removal of the small, hydrophobic leucine side chain of L329 led to greater activity reduction than mutating L324. The isobutyl group of L329 is observed in the cocrystal structure to stack between the terminal and penultimate bases of the DNA.

Mutations targeting the third class of residues, those which contact the DNA substrate distal to the scissile phosphodiester bond (Q384A and N385A), resulted in attenuation of activity ranging from 23 to 60% of wild-type levels, depending on the nature of substrates and mutations. The level of activity reduction of this class of mutants is generally lower for the mismatched duplex than for either the single-stranded or matched duplex forms of the substrate (see Table 2). A double mutant targeting both of these amide residues has activity 3-fold lower than that predicted by simple additive effects (8.2% vs 3.3%).

*Effects of Metal on 3′−5′ Exonuclease Activity.* One of the most important parameters for PCR optimization is the nature and concentration of the divalent metal ion cofactor. Both $Mn^{2+}$ and $Mg^{2+}$ can be used as divalent metal cations by DNA pols to catalyze 5′−3′ primer extension (*18*). However, the fidelity is lower for $Mn^{2+}$ activation than for $Mg^{2+}$ activation (*43*). We therefore measured the 3′−5′ exonuclease activity of the CS5 pol wild-type chimera and

Table 1: Candidate Residues for Mutation in the *Tma* pol 3′−5′ Exonuclease Domain of CS5 Chimeric DNA Polymerase

| class | residue in *Tma* pol[a] | residue in Klenow fragment | motif | function | mutation |
|---|---|---|---|---|---|
| ligands to the metal ions | Asp323 | Asp355 | Exo I | chelates metal ion A | Glu or Ala |
| | Glu325 | Glu357 | Exo I | chelates metal ion A | Asp or Ala |
| | Asp389 | Asp424 | Exo II | indirectly chelates metal ion B | Glu |
| substrate contacts at the 3′ terminus | Leu324 | Thr356 | Exo I | no interactions with substrate; located between essential carboxylates D323 and E325 | Gln, His, Glu, Lys, Asn, or Asp |
| | Tyr464 | Tyr497 | Exo III | H-bond to scissile phosphodiester | Ala |
| | Leu329 | Leu361 | Exo I | stacks between $P_n$ and $P_{n-1}$ | Ala |
| upstream contacts with the substrate sugar−phosphate backbone | Gln384 | Gln419 | Exo II | H-bond to phosphodiester between $P_{n-1}$ and $P_{n-2}$ | Ala |
| | Asn385 | Asn420 | Exo II | H-bond to 4′-O of $P_{n-1}$ | Ala |

[a] The residues were suggested by molecular modeling to be involved in catalysis and/or substrate binding in the 3′−5′ exonuclease domain.

Table 2: 3′−5′ Exonuclease Activity of Wild-Type and Mutant Derivatives of CS5 pol

| | single-stranded | | double-stranded, matched | | double-stranded, mismatched | |
|---|---|---|---|---|---|---|
| enzyme | specific activity (units/pmol) | %[a] | specific activity (units/pmol) | %[a] | specific activity (units/pmol) | %[a] |
| CS5 | 9.9 | 100.0 | 11.3 | 100.0 | 16.6 | 100.0 |
| CS6 | <0.001 | <0.01 | <0.001 | <0.01 | <0.001 | <0.01 |
| D323E | <0.001 | <0.01 | <0.001 | <0.01 | <0.001 | <0.01 |
| E325D | <0.001 | <0.01 | <0.001 | <0.01 | <0.001 | <0.01 |
| D323E/E325D | <0.001 | <0.01 | <0.001 | <0.01 | <0.001 | <0.01 |
| D389E | 1.6 | 16.2 | 1.9 | 16.5 | 4.9 | 29.3 |
| L324Q | 2.7 | 27.2 | 3.6 | 32.2 | 6.9 | 41.6 |
| L324H | 3.4 | 34.0 | 3.9 | 35.1 | 7.2 | 43.7 |
| L324E | 4.8 | 48.2 | 4.1 | 36.7 | 7.4 | 44.9 |
| L324D | 6.1 | 61.3 | 4.4 | 39.4 | 9.5 | 57.3 |
| L324K | 3.4 | 34.5 | 5.0 | 44.9 | 9.2 | 55.7 |
| L324N | 4.0 | 40.5 | 5.3 | 47.0 | 11.1 | 66.8 |
| Y464A | 0.031 | 0.31 | 0.057 | 0.50 | 0.090 | 0.54 |
| L329A | 1.1 | 10.7 | 0.9 | 7.8 | 3.2 | 19.3 |
| Q384A | 2.3 | 22.9 | 2.7 | 23.7 | 7.6 | 45.8 |
| N385A | 3.5 | 35.6 | 4.3 | 38.6 | 10.6 | 63.8 |
| Q384A/N385A | 0.4 | 3.7 | 0.5 | 4.1 | 1.8 | 10.9 |

[a] Percent relative to that of wild-type CS5 pol (defined as 100%).

Table 3: Comparison of 3′−5′ Exonuclease Activities in $Mg^{2+}$ and $Mn^{2+}$

| | single-stranded | | double-stranded, matched | | double-stranded, mismatched | |
|---|---|---|---|---|---|---|
| enzyme | specific activity (units/pmol) | % activity [$Mg^{2+}/Mn^{2+}$] | specific activity (units/pmol) | % activity [$Mg^{2+}/Mn^{2+}$] | specific activity (units/pmol) | % activity [$Mg^{2+}/Mn^{2+}$] |
| CS5 | 0.67 | 6.8 | 1.2 | 10.2 | 1.6 | 9.4 |
| D389E | 0.19 | 11.8 | 0.15 | 7.9 | 0.23 | 4.7 |
| L329A | 0.028 | 2.5 | 0.086 | 9.6 | 0.17 | 5.2 |
| Q384A | 0.24 | 10.3 | 0.19 | 7.1 | 0.36 | 4.8 |
| N385A | 0.18 | 3.8 | 0.16 | 5.1 | 0.41 | 3.9 |
| Q384A/N385A | 0.013 | 3.3 | 0.035 | 9.1 | 0.077 | 4.3 |

several of the mutant enzymes in $Mg^{2+}$-containing buffer to augment the studies in the $Mn^{2+}$-optimized buffer. The chimera CS5 pol 3′−5′ exonuclease activity was lower in $Mg^{2+}$-containing buffer than in $Mn^{2+}$-containing buffer [∼10-fold lower for double-stranded DNA and ∼15-fold lower for single-stranded DNA (Table 3)]. Like CS5 pol, the mutants also had reduced 3′−5′ exonuclease activity in $Mg^{2+}$ compared to $Mn^{2+}$. However, the activity on different substrates varied for the different mutants. For PCR, it is preferable to have weak proofreading degradation of single-stranded DNA relative to double-stranded DNA.

*3′−5′ Exonuclease Enzyme Kinetics.* To gain a better understanding of the catalytic mechanism of the *Tma* pol proofreading domain and how it may differ from its mesophilic counterpart, *E. coli* pol I, we determined the kinetic parameters for the wild-type chimera and the attenuated 3′−5′ exonuclease mutants. Oligonucleotide substrate NJS98 was used to determine kinetic parameters, either single-stranded or annealed to NJS99B. The homopolymeric sequence ensured uniform degradation rates since the sequence context did not change upon degradation. The fact that multiple degradative events were considered in which the product of removal served as a further substrate thus increased assay linearity and sensitivity. This assay format thus provided a dynamic range much greater than that discussed above for relative activity determination but

Table 4: 3′−5′ Exonuclease Activity Kinetic Parameters for Wild-Type CS5 pol and Selected Mutants

| | single-stranded | | | double-stranded | | | |
|---|---|---|---|---|---|---|---|
| enzyme | $K_M$ ($\mu$M) | $k_{cat}$ ($s^{-1}$) | $k_{cat}/K_M$ ($\mu M^{-1}\ s^{-1}$) | $K_M$ (nM) | $k_{cat}$ ($s^{-1}$) | $k_{cat}/K_M$ ($\mu M^{-1}\ s^{-1}$) | $(k_{cat}/K_M)_{double-stranded}/(k_{cat}/K_M)_{single-stranded}$ |
| CS5 | 0.74 | 2.34 | 3.16 | 5.66 | 0.95 | 168.5 | 53.3 |
| D389E | 1.34 | 0.098 | 0.07 | 7.1 | 0.12 | 17.5 | 238.6 |
| L329A | 2.3 | 0.036 | 0.02 | 5.45 | 0.032 | 5.9 | 377.4 |
| Q384A | 1.94 | 0.15 | 0.08 | 5.93 | 0.16 | 26.1 | 346.1 |
| N385A | 1.56 | 0.36 | 0.23 | 5.88 | 0.45 | 76.0 | 326.2 |
| Q384A/N385A | 1.54 | 0.014 | 0.01 | 4.23 | 0.030 | 7.1 | 769.7 |
| Klenow fragment | 0.12 | 0.14 | 1.19 | 3.2 | 0.0036 | 1.10 | 0.9 |

precluded examination of the 3′ terminally mismatched duplex since the mismatch would define only the first phosphodiester target.

Because the kinetic behavior of the Klenow fragment has been extensively studied, we first measured the kinetic parameters of the Klenow fragment using previously reported buffer conditions (*44*) to validate our assay format. Using our fluorescent, partially homopolymeric substrate (NJS98), our results were consistent with previously published data for the Klenow fragment for single-stranded substrate (*44*) and for double-stranded substrate (*45*) (Table 4). Furthermore, our results confirm that the Klenow fragment utilizes both single-stranded and double-stranded forms of substrate with equal efficiency due to compensating changes in the $k_{cat}$ and $K_M$ values. Whereas catalysis is faster on single-stranded DNA as opposed to double-stranded DNA, binding is weaker for the former.

The kinetics of the *Tma* pol 3′−5′ exonuclease domain in the CS5 chimera exhibited several differences from those of the Klenow fragment. The $K_M$ of CS5 pol (Table 4) for double-stranded DNA is also in the nanomolar range (5.7 ± 1.9 nM), while the $K_M$ for the NJS98 single-stranded DNA (740 ± 280 nM) is approximately 6-fold higher than that measured for the Klenow fragment. More dramatically, the maximal rate of 3′−5′ exonucleolysis was much faster for CS5 pol and had similar $k_{cat}$ values for single-stranded DNA and double-stranded DNA (0.95 ± 0.08 $s^{-1}$ for double-stranded DNA and 2.3 ± 0.1 $s^{-1}$ for single-stranded DNA). Compared to that of the Klenow fragment, the $k_{cat}$ of CS5 was ~17-fold higher for single-stranded DNA and 263-fold higher for double-stranded DNA. The resulting specificity constant, $k_{cat}/K_M$, indicates a greater than 50-fold preference for the double-stranded substrate over the single-stranded substrate rather than equal efficiency on both substrates observed with the Klenow fragment.

To be able to predict proofreading behavior at any substrate concentration, as well as to understand if the activity reduction observed for the various mutants stems from effects on substrate binding or on catalysis, the kinetic parameters were determined for representatives from each of the three classes of mutants (Table 4). The mutations had almost no effect on the $K_M$ value for double-stranded DNA and increased the $K_M$ for single-stranded DNA by a factor of only 2−3 when compared to that of the parent CS5 pol. The effect of the mutations on the $k_{cat}$ value for both forms of the substrate was greater: 2−30-fold decrease for double-stranded DNA and 6−160-fold decrease for single-stranded DNA. The resulting specificity constants ($k_{cat}/K_M$) of the mutants, for double-stranded DNA versus single-stranded DNA, indicate an increase in the strength of the preference for the double-stranded form of the DNA substrate compared to the parent enzyme.

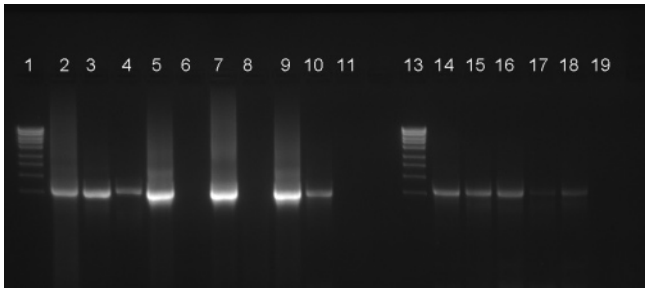


FIGURE 2: RT/PCR results. RT/PCR with $10^4$ copies/reaction of HIV-1 RNA transcript with 50 units of enzyme. The specific product is 1.7 kb in length: lanes 1 and 13, MassRuler DNA Ladder, High Range; lanes 2−11, D323E/E325D, D389E, L324Q, L329A, Y464A, Q384A, N385A, Q384A/N385A, CS6, and CS5, respectively; lanes 14−19, RT/PCR with $10^4$ copies/reaction of HIV-1 RNA transcript with either CS5 or CS6 or with a blend of CS5 and CS6; lane 14, 50 units of CS6; lane 15, 2 units of CS5 and 48 units of CS6; lane 16, 5 units of CS5 and 45 units of CS6; lane 17, 10 units of CS5 and 40 units of CS6; lane 18, 25 units of CS5 and 25 units of CS6; and lane 19, 50 units of CS5.

*RT/PCR Amplification*. The ability of the mutant DNA polymerases to generate 1.7 kb amplicons from HIV-1 RNA transcript was evaluated (Figure 2). In this system, essentially no product was observed when the DNA polymerase had high levels of proofreading activity, e.g., the CS5 pol parent enzyme alone. Amplification by an enzyme lacking proofreading activity, e.g., CS6 pol alone, yielded a minimal specific product. The blending of various concentrations of CS5 pol and CS6 pol yielded small amounts of specific products. The performance of six of eight of the mutants was at least equivalent to that of the control chimera CS6 or any of the enzyme blends, while three performed substantially better (L329A, Q384A, and Q384A/N385A).

## DISCUSSION

The goal of this study was to rationally design mutants of a thermostable chimeric DNA polymerase to reduce, but not eliminate, the 3′−5′ exonuclease activity. Such mutants, it was hoped, would function as a single enzyme in RT/PCR or PCR applications that normally require blending 3′−5′ exonuclease-containing and 3′−5′ exonuclease-deficient DNA polymerases to achieve low levels of proofreading activity. The consequence of modifying the previously produced chimeric construct was to achieve the first DNA polymerases with efficient reverse transcriptase and 3′−5′ exonuclease (proofreading) activity.

The first category of mutations targeted the metal ligating residues of the active site. While it had been shown that

removal of the carboxylate group from the absolutely conserved glutamate and aspartate residues in motifs Exo I and II completely eliminated 3′−5′ exonuclease activity (*44*, *46*), we found that even conservative, length-modifying mutations to metal ion A ligators D323E or E325D eliminated 3′−5′ exonuclease activity below the detectable levels of our assay. The equivalent acidic side chain length mutations have not been described for *E. coli* pol I. On the other hand, similar length-modulating changes to metal ion B ligator D389E resulted in the desired partial activity reduction. These disparate tolerances for such mutations may be attributed to differences in the nature of metal ligation by these residues. The D323 and E325 residues ligate metal ion A directly, while residue D389 is coordinated via two water molecules to metal ion B. This indirect ligation could offer more tolerance to the placement of the carboxylate group. The homologous mutation to metal ion B ligator D424E in *E. coli* pol I had a similar modulating effect (*44*).

The second category of mutations was directed at three residues located near the active site but not involved in metal coordination: Y464, L329, and L324. There are conflicting data about the role of the Y464 residue (*42*, *44*, *47*). Unlike the analogous mutation in the Klenow fragment which resulted in an only modest reduction in activity (*42*), we find that the Y464A mutation completely eliminates the 3′−5′ exonuclease activity and is consistent with the proposed role of the phenolic OH hydrogen bonding to the attacking $OH^-$, as seen in earlier cocrystal structures (*25*, *48*). We cannot rule out the possibility that this amino acid substitution causes subtle structural changes which are critical in the 3′−5′ exonuclease active site of *Tma* pol. The second residue in this category to be targeted for mutagenesis, L324, is not conserved among the pol A family polymerases. With the intention of only slightly perturbing the geometric arrangement of the flanking liganding groups, we mutated the small, neutral side chain of L324 to a number of charged or polar residues. Such mutations indeed resulted in a very modest reduction in 3′−5′ exonuclease activity similar to earlier reports for the *Archaea* DNA polymerase from *Thermococcus kodakaraensis* KOD1 (*49*). The side chain of the final residue mutated in this category, L329, is inserted between the terminal and penultimate bases. The homologous mutation in *E. coli* pol I (L361A) led to a similar modest reduction in activity, it being, however, much stronger for double-stranded DNA than for single-stranded DNA. In contrast, this mutation in *Tma* pol shows comparable activity reduction on double- and single-stranded substrates (*42*). For the third category of mutations, the greater than expected activity reduction for removal of both amide side chains of Q384 and N385 indicates that the substrate interactions contributed by these two neighboring side chains are cooperative.

The structural studies of the Klenow fragment and other DNA polymerases have been complemented not only by extensive site-directed mutagenesis but also by kinetic characterizations to confirm the role of residues and clarify the reaction mechanism (*22*, *42*, *45*, *50*−*55*). In the course of our study, we have characterized the steady-state kinetics of 3′−5′ exonuclease activity of both the wild-type and mutant enzymes from *Tma*. Like that of the Klenow fragment, the $K_M$ value of *Tma* pol for double-stranded DNA is similar for both the 5′−3′ primer extension and 3′−5′ exonuclease activities, consistent with the model in which binding of DNA with a recessed 3′ terminus occurs initially in the DNA polymerase domain. If extension is slow due to the presence of a mismatch or the lack of the next correct dNTP, then the primer is shuttled down to the 3′−5′ exonuclease domain where hydrolytic removal of the terminal nucleoside is catalyzed. This strand transfer is proposed to be rate-limiting for the Klenow fragment because the $k_{cat}$ for double-stranded DNA is much slower than for single-stranded DNA. In *Tma* pol, the $k_{cat}$ value for double-stranded DNA is almost as fast as for single-stranded DNA, and both are faster than for the Klenow fragment. Thus, *Tma* pol appears to still bind double-stranded DNA in the polymerase active site but shuttles it much faster than the Klenow fragment under the assay conditions that were tested. This faster strand transfer could be due to a faster rate of release from the DNA pol active site or a faster strand accepting rate on the part of the proofreading active site. Examination of the kinetic behavior of the two enzymes on single-stranded DNA provides a glimpse into the source of this kinetic acceleration. The $k_{cat}$ on single-stranded DNA of *Tma* pol is roughly ∼17-fold faster than that of the Klenow fragment. Assuming that this rate increase reflects faster strand acceptance by the proofreading domain, it implies that the additional 15-fold rate acceleration for double-stranded DNA substrate by *Tma* pol over *E. coli* pol I derives from a 15-fold faster strand release rate from the DNA polymerase domain. Perhaps the more hydrophobic nature and increased length of the loop of residues 443−451 in the *Tma* pol 3′−5′ exonuclease domain (Figure 1a) account for some of these differences in kinetic behavior from the Klenow fragment.

Determination of the kinetic parameters for these mutants reveals a much greater effect on $k_{cat}$ than on $K_M$, implying that these interactions are more important with the transition state form of the substrate than the ground state. Perhaps formation of the interactions and orientation of the DNA substrate, as observed in the cocrystal structure, reflect the rate-limiting step in the catalysis of hydrolysis.

Several of the new designer enzymes with modulated proofreading activity function to replace the conventional mixture of DNA polymerases in the cDNA synthesis and amplification of a 1.7 kb RNA target. Following misincorporation by a nonproofreading DNA polymerase during either reverse transcription or PCR amplification, the terminally mismatched primer is either extended slowly, thus locking in the mistake, or not further extended, thus lowering cDNA and/or amplification efficiency. A proofreading proficient DNA polymerase can remove the mismatch, thus improving fidelity and efficiency. The benefit of proofreading depends on the rate of misincorporation, the length of the amplicon, and the relative mismatch extension rate. In the case of 3′−5′ exonuclease-containing and 3′−5′ exonuclease-deficient blends of DNA polymerases, a poorly extendable mismatch must dissociate from the predominant 3′−5′ exonuclease-deficient DNA polymerase and bind to the minority 3′-5′ exonuclease-containing DNA polymerase before it can finally be proofread. With a modulated proofreading thermostable DNA polymerase, the correction of a 3′ terminal mismatch on a primer following misincorporation can occur intramolecularly rather than intermolecularly without the potential detrimental effects of full proofreading activity. Indeed, three of the eight mutants with reduced 3′−5′ exonuclease activity had substantially im-

proved RT/PCR activity (L329A, Q384A, and Q384A/N385A). This is the first demonstration of thermoactive and thermostable pol A DNA polymerases containing 3′−5′ exonucleolytic (proofreading) activity that are capable of efficient reverse transcription and single-enzyme RT/PCR.

Although we measure an ∼50-fold higher catalytic efficiency on double-stranded DNA than on single-stranded DNA, which is favorable for PCR, we have found that it still is beneficial to protect the primers for PCR applications since there is a huge excess of the single-stranded primer over the concentration of the primed template. This is particularly true for RT/PCR applications where there is an extended incubation time during the reverse transcription step. We have found that penultimate 2′-amino groups, 2′-OH groups, or 2′-O-methyl groups afford protection against 3′−5′ exonuclease degradation while allowing efficient primer extension.

The creation of an accurate homology model of the *Tma* pol proofreading domain based on the Klenow fragment structure allowed us to successfully identify modulating mutations for the 3′−5′ exonuclease activity. Kinetic characterizations of the wild-type chimera as well as some differences in the effect of mutating certain residues point to differences in the mechanism of *Tma* pol versus its mesophilic counterpart. Additionally, this work demonstrates the success of a rational design approach to creating modulated proofreading DNA polymerases which can be utilized in a highly sensitive long RT/PCR amenable to the clinical diagnostic setting.

## ACKNOWLEDGMENT

We thank K. Bauer for generous assistance with protein purification and the Department of Core Chemistry for the synthesis of oligonucleotides.

## REFERENCES

1. Barnes, W. M. (1994) PCR amplification of up to 35-kb DNA with high fidelity and high yield from λ bacteriophage templates, *Proc. Natl. Acad. Sci. U.S.A. 91*, 2216−20.
2. Roberts, J. D., Bebenek, K., and Kunkel, T. A. (1988) The accuracy of reverse transcriptase from HIV-1, *Science 242*, 1171−3.
3. Gelfand, D. H., and White, T. J. (1990) Thermostable DNA Polymerases, in *PCR Protocols: A Guide to Methods and Applications* (Innis, M. A., Gelfand, D. H., Sninsky, J. J., and White, T. J., Eds.) pp 129−41, Academic Press, San Diego.
4. Eckert, K. A., and Kunkel, T. A. (1990) High fidelity DNA synthesis by the *Thermus aquaticus* DNA polymerase, *Nucleic Acids Res. 18*, 3739−44.
5. Cline, J., Braman, J. C., and Hogrefe, H. H. (1996) PCR fidelity of *pfu* DNA polymerase and other thermostable DNA polymerases, *Nucleic Acids Res. 24*, 3546−51.
6. Cheng, S., Fockler, C., Barnes, W. M., and Higuchi, R. (1994) Effective amplification of long targets from cloned inserts and human genomic DNA, *Proc. Natl. Acad. Sci. U.S.A. 91*, 5695−9.
7. Kunkel, T. A. (1988) Exonucleolytic proofreading, *Cell 53*, 837−40.
8. Kong, H., Kucera, R. B., and Jack, W. E. (1993) Characterization of a DNA polymerase from the hyperthermophile archaea *Thermococcus litoralis*. Vent DNA polymerase, steady-state kinetics, thermal stability, processivity, strand displacement, and exonuclease activities, *J. Biol. Chem. 268*, 1965−75.
9. Jannasch, H. W., Wirsen, C. O., Molyneaux, S. J., and Langworthy, T. A. (1992) Comparative physiological studies on hyperthermophilic archaea isolated from deep-sea hot vents with emphasis on *Pyrococcus* strain GB-D, *Appl. Environ. Microbiol. 58*, 3472−81.
10. Longo, M. C., Berninger, M. S., and Hartley, J. L. (1990) Use of uracil DNA glycosylase to control carry-over contamination in polymerase chain reactions, *Gene 93*, 125−8.
11. Lasken, R. S., Schuster, D. M., and Rashtchian, A. (1996) Archaebacterial DNA polymerases tightly bind uracil-containing DNA, *J. Biol. Chem. 271*, 17692−6.
12. Fogg, M. J., Pearl, L. H., and Connolly, B. A. (2002) Structural basis for uracil recognition by archaeal family B DNA polymerases, *Nat. Struct. Biol. 9*, 922−7.
13. Myers, T. (1999) Recent Advances in High-Temperature Reverse Transcription and PCR, in *PCR Applications: Protocols for Functional Genomics* (Innis, M. A., Gelfand, D. H., and Sninsky, J. J., Eds.) pp 141−52, Academic Press, San Diego.
14. Skerra, A. (1992) Phosphorothioate primers improve the amplification of DNA sequences by DNA polymerases with proofreading activity, *Nucleic Acids. Res. 20*, 3551−4.
15. Brautigam, C. A., and Steitz, T. A. (1998) Structural principles for the inhibition of the 3′−5′ exonuclease activity of *Escherichia coli* DNA polymerase I by phosphorothioates, *J. Mol. Biol. 277*, 363−77.
16. Tindall, K. R., and Kunkel, T. A. (1988) Fidelity of DNA synthesis by the *Thermus aquaticus* DNA polymerase, *Biochemistry 27*, 6008−13.
17. Lawyer, F. C., Stoffel, S., Saiki, R. K., Myambo, K., Drummond, R., and Gelfand, D. H. (1989) Isolation, characterization, and expression in *Escherichia coli* of the DNA polymerase gene from *Thermus aquaticus*, *J. Biol. Chem. 264*, 6427−37.
18. Myers, T. W., and Gelfand, D. H. (1991) Reverse transcription and DNA amplification by a *Thermus thermophilus* DNA polymerase, *Biochemistry 30*, 7661−6.
19. Meng, Q., Wong, C., Rangachari, A., Tamatsukuri, S., Sasaki, M., Fiss, E., Cheng, L., Ramankutty, T., Clarke, D., Yawata, H., Sakakura, Y., Hirose, T., and Impraim, C. (2001) Automated multiplex assay system for simultaneous detection of hepatitis B virus DNA, hepatitis C virus RNA, and human immunodeficiency virus type 1 RNA, *J. Clin. Microbiol. 39*, 2937−45.
20. Smith, E. S., Li, A. K., Wang, A. M., Gelfand, D. H., and Myers, T. (2003) Amplification of RNA: High-temperature Reverse Transcription and DNA Amplification with a Magnesium-activated Thermostable DNA Polymerase, in *PCR primer: A Laboratory Manual* (Dieffenbach, C. W., and Dveksler, G. S., Eds.) pp 211−219, Cold Spring Harbor Laboratory Press, Cold Spring Harbor, NY.
21. Kim, Y., Eom, S. H., Wang, J., Lee, D. S., Suh, S. W., and Steitz, T. A. (1995) Crystal structure of *Thermus aquaticus* DNA polymerase, *Nature 376*, 612−6.
22. Joyce, C. M., and Steitz, T. A. (1994) Function and structure relationships in DNA polymerases, *Annu. Rev. Biochem. 63*, 777−822.
23. Patel, P. H., Suzuki, M., Adman, E., Shinkai, A., and Loeb, L. A. (2001) Prokaryotic DNA polymerase I: Evolution, structure, and "base flipping" mechanism for nucleotide selection, *J. Mol. Biol. 308*, 823−37.
24. Brautigam, C. A., and Steitz, T. A. (1998) Structural and functional insights provided by crystal structures of DNA polymerases and their substrate complexes, *Curr. Opin. Struct. Biol. 8*, 54−63.
25. Beese, L. S., and Steitz, T. A. (1991) Structural basis for the 3′−5′ exonuclease activity of *Escherichia coli* DNA polymerase I: A two metal ion mechanism, *EMBO J. 10*, 25−33.
26. Freemont, P. S., Friedman, J. M., Beese, L. S., Sanderson, M. R., and Steitz, T. A. (1988) Cocrystal structure of an editing complex of Klenow fragment with DNA, *Proc. Natl. Acad. Sci. U.S.A. 85*, 8924−8.
27. Derbyshire, V., Freemont, P. S., Sanderson, M. R., Beese, L., Friedman, J. M., Joyce, C. M., and Steitz, T. A. (1988) Genetic and crystallographic studies of the 3′-5′-exonucleolytic site of DNA polymerase I, *Science 240*, 199−201.
28. Ollis, D. L., Brick, P., Hamlin, R., Xuong, N. G., and Steitz, T. A. (1985) Structure of large fragment of *Escherichia coli* DNA polymerase I complexed with dTMP, *Nature 313*, 762−6.
29. Curley, J. F., Joyce, C. M., and Piccirilli, J. A. (1997) Functional evidence that the 3′-5′ exonuclease domain of *E. coli* DNA polymerase I employs a divalent metal ion in leaving group stabilization, *J. Am. Chem. Soc. 119*, 12691−2.
30. Abramson, R. D. (1995) DNA Polymerases, in *PCR Strategies* (Innis, M. S., Gelfand, D., and Sninsky, J. J., Eds.) pp 39−57, Academic Press, San Diego.
31. Villbrandt, B., Sobek, H., Frey, B., and Schomburg, D. (2000) Domain exchange: Chimeras of *Thermus aquaticus* DNA poly-

merase, *Escherichia coli* DNA polymerase I and *Thermotoga neapolitana* DNA polymerase, *Protein Eng. 13*, 645−54.
32. Sauer, S., Gelfand, D. H., Boussicault, F., Bauer, K., Reichert, F., and Gut, I. G. (2002) Facile method for automated genotyping of single nucleotide polymorphisms by mass spectrometry, *Nucleic Acids Res. 30*, e22.
33. Beaucage, S. L., and Caruthers, M. H. (1981) Deoxynucleoside phosphoramidites: A new class of key intermediates for deoxypolynucleotide synthesis, *Tetrahedron Lett. 22*, 1859−62.
34. Broger, C. Personal communication.
35. Gerber, P. R., and Muller, K. (1995) MAB, a generally applicable molecular force field for structure modelling in medicinal chemistry, *J. Comput.-Aided Mol. Des. 9*, 251−68.
36. Higuchi, R., Krummel, B., and Saiki, R. K. (1988) A general method of in vitro preparation and specific mutagenesis of DNA fragments: Study of protein and DNA interactions, *Nucleic Acids Res. 16*, 7351−67.
37. Lawyer, F. C., Stoffel, S., Saiki, R. K., Chang, S. Y., Landre, P. A., Abramson, R. D., and Gelfand, D. H. (1993) High-level expression, purification, and enzymatic characterization of full-length *Thermus aquaticus* DNA polymerase and a truncated form deficient in 5′ to 3′ exonuclease activity, *PCR Methods Appl. 2*, 275−87.
38. Marti-Renom, M. A., Stuart, A. C., Fiser, A., Sanchez, R., Melo, F., and Sali, A. (2000) Comparative protein structure modeling of genes and genomes, *Annu. Rev. Biophys. Biomol. Struct. 29*, 291−325.
39. Bernad, A., Blanco, L., Lazaro, J. M., Martin, G., and Salas, M. (1989) A conserved 3′−5′ exonuclease active site in prokaryotic and eukaryotic DNA polymerases, *Cell 59*, 219−28.
40. Bowie, J. U., Zhang, K., Wilmanns, M., and Eisenberg, D. (1996) Three-dimensional profiles for measuring compatibility of amino acid sequence with three-dimensional structure, *Methods Enzymol. 266*, 598−616.
41. Luthy, R., Bowie, J. U., and Eisenberg, D. (1992) Assessment of protein models with three-dimensional profiles, *Nature 356*, 83−5.
42. Derbyshire, V., Pinsonneault, J. K., and Joyce, C. M. (1995) Structure−function analysis of 3′→5′-exonuclease of DNA polymerases, *Methods Enzymol. 262*, 363−85.
43. Beckman, R. A., Mildvan, A. S., and Loeb, L. A. (1985) On the fidelity of DNA replication: Manganese mutagenesis *in vitro*, *Biochemistry 24*, 5810−7.
44. Derbyshire, V., Grindley, N. D., and Joyce, C. M. (1991) The 3′−5′ exonuclease of DNA polymerase I of *Escherichia coli*: Contribution of each amino acid at the active site to the reaction, *EMBO J. 10*, 17−24.
45. Kuchta, R. D., Benkovic, P., and Benkovic, S. J. (1988) Kinetic mechanism whereby DNA polymerase I (Klenow) replicates DNA with high fidelity, *Biochemistry 27*, 6716−25.
46. Reha-Krantz, L. J., and Nonay, R. L. (1993) Genetic and biochemical studies of bacteriophage T4 DNA polymerase 3′→5′-exonuclease activity, *J. Biol. Chem. 268*, 27100−8.
47. Lam, W. C., Van der Schans, E. J., Joyce, C. M., and Millar, D. P. (1998) Effects of mutations on the partitioning of DNA substrates between the polymerase and 3′−5′ exonuclease sites of DNA polymerase I (Klenow fragment), *Biochemistry 37*, 1513−22.
48. Beese, L. S., Derbyshire, V., and Steitz, T. A. (1993) Structure of DNA polymerase I Klenow fragment bound to duplex DNA, *Science 260*, 352−5.
49. Kuroita, T., Matsumura, H., Yokota, N., Kitabayashi, M., Hashimoto, H., Inoue, T., Imanaka, T., and Kai, Y. (2005) Structural mechanism for coordination of proofreading and polymerase activities in archaeal DNA polymerases, *J. Mol. Biol. 351*, 291−8.
50. Eger, B. T., and Benkovic, S. J. (1992) Minimal kinetic mechanism for misincorporation by DNA polymerase I (Klenow fragment), *Biochemistry 31*, 9227−36.
51. Mizrahi, V., Benkovic, P., and Benkovic, S. J. (1986) Mechanism of DNA polymerase I: Exonuclease/polymerase activity switch and DNA sequence dependence of pyrophosphorolysis and misincorporation reactions, *Proc. Natl. Acad. Sci. U.S.A. 83*, 5769−73.
52. Otto, M. R., Bloom, L. B., Goodman, M. F., and Beechem, J. M. (1998) Stopped-flow fluorescence study of precatalytic primer strand base-unstacking transitions in the exonuclease cleft of bacteriophage T4 DNA polymerase, *Biochemistry 37*, 10156−63.
53. Reha-Krantz, L. J., Marquez, L. A., Elisseeva, E., Baker, R. P., Bloom, L. B., Dunford, H. B., and Goodman, M. F. (1998) The proofreading pathway of bacteriophage T4 DNA polymerase, *J. Biol. Chem. 273*, 22969−76.
54. Beechem, J. M., Otto, M. R., Bloom, L. B., Eritja, R., Reha-Krantz, L. J., and Goodman, M. F. (1998) Exonuclease-polymerase active site partitioning of primer-template DNA strands and equilibrium $Mg^{2+}$ binding properties of bacteriophage T4 DNA polymerase, *Biochemistry 37*, 10144−55.
55. Bloom, L. B., Otto, M. R., Eritja, R., Reha-Krantz, L. J., Goodman, M. F., and Beechem, J. M. (1994) Pre-steady-state kinetic analysis of sequence-dependent nucleotide excision by the 3′-exonuclease activity of bacteriophage T4 DNA polymerase, *Biochemistry 33*, 7576−86.

BI0609117